*Laser Chem.*, 1998, Vol. 17, pp. 185–190
Reprints available directly from the publisher
Photocopying permitted by license only

© 1998 OPA (Overseas Publishers Association) N.V.
Published by license under
the Harwood Academic Publishers imprint,
part of The Gordon and Breach Publishing Group.
Printed in India.

# PHOTOFRAGMENTATION OF $Cl_2$ AT 308 NM

PETER C. SAMARTZIS, THEODOSIA GOUGOUSI
and THEOFANIS N. KITSOPOULOS*

*Department of Chemistry, University of Crete and Institute of Electronic Structure and Laser, Foundation for Research and Technology-Hellas, 711 10 Heraklion-Crete, Greece*

*(Received 10 October 1997)*

The velocity distributions for the $Cl(^2P_{3/2})$ and $Cl(^2P_{1/2})$ photofragments produced by the photolysis of $Cl_2$ at 308 nm are measured using ion imaging. The angular distributions yield anisotropy parameters of $\beta(^2P_{3/2}) = -1.00 \pm 0.05$, $\beta(^2P_{1/2}) = -0.95 \pm 0.05$, suggesting that $Cl(^2P_{1/2})$ is essentially produced via non-adiabatic curve crossing between the $1_u$ and the $0_u^+$ excited electronic states.

*Keywords:* Photofragmentation; photodissociation; chlorine; ultraviolet; laser

## INTRODUCTION

The ultraviolet absorption spectrum of molecular chlorine between 250 and 450 nm has been attributed to transitions between the $Cl_2(X^1\Sigma_g)$ ground electronic state and the purely repulsive $^1\Pi_u$ and $B^3\Pi_u$ excited electronic states. A correlation diagram between the atomic states of free Cl and the molecular electronic states of $Cl_2$ has been reported by Mulliken [1], Herzberg [2], Li *et al.* [3] and Matsumi *et al.* [4], according to which the strong spin-orbit interaction in atomic chorine mandates a Hund's case (*c*) description of $Cl_2$ [5]. Consequently, the notation for the above molecular electronic states

* Corresponding author.

are $0_g^+(X^1\Sigma_g), 1_u(^1\Pi_u)$, these two states correlating to $Cl(^2P_{3/2}) + Cl(^2P_{3/2})$ and $0_u^+(B^3\Pi_u)$ a state that correlates to $Cl(^2P_{3/2}) + Cl(^2P_{1/2})^2$. In the remaining manuscript we will use Cl and $Cl^*$ to denote $Cl(^2P_{3/2})$ and $Cl(^2P_{1/2})$ respectively, following the same notation used by Matsumi *et al.* [4].

The nature of the transition probability, coupled with the lifetime and the rotational period of the excited state, have a direct consequence to the angular distribution $I(\theta)$ of the photofragments, which is described by the equation [6, 7]

$$I(\theta) = \frac{1}{4\pi}(1 + \beta P_2(\cos\theta)) \tag{1}$$

where $\beta$ is called the anisotropy parameter ($-1 \leq \beta \leq 2$) and $P_2(\cos\theta)$ is the second Legendre polynomial. For a prompt dissociation $\beta = -1$ if the transition is perpendicular ($\Delta\Omega = \pm 1$) and $\beta = 2$ if a parallel transition ($\Delta\Omega = 0$) is involved. Clearly, the shape of photofragment angular distribution can provide useful information concerning the nature of the $Cl_2$ photodissociation process in this near ultraviolet region (275 to 450 nm). Such studies in the vicinity of the absorption maximum ($\sim 330$ nm) have been reported by a number of groups [3, 4, 8–11]. In this report we present our results concerning the velocity distributions (speed and angle) of the Cl and $Cl^*$ photofragments following the photolysis of $Cl_2$ at 308 nm using an ion imaging technique [12–14].

## EXPERIMENTAL

The apparatus has been described in detail elsewhere [15]. Briefly, a gas sample containing 5% $Cl_2$ in He, is expanded into the source vacuum chamber via a home-build piezoelectrically-actuated pulsed-molecular beam operating at 20 Hz. The beam which is skimmed and collimated, is intersected at right angles by two counter propagating laser beams generated by an excimer-pumped (Lumonics HyperX400, operating with XeCl) pulsed-dye laser (ELTO LT1233, operating with Coumarin 480), using a BBO crystal. Part of the 308 nm laser light from the excimer is split, linearly polarized, and used for the photodissociation

of $Cl_2$. The Cl-atom photofragments are ionized using (2 + 1) REMPI, and the ions produced are accelerated towards a home-built ion-imaging detector. Images appearing on the detector anode are recorded using a CCD video camera. Ions of different masses are separated by time-of-flight during their field-free trajectory on route to the detector.

Following the pioneering work of Eppink and Parker [16] we have adopted the *velocity imaging* technique as a major modification in our experimental apparatus. The modification involves replacing the uniform extraction field assembly which consisted of a repeller and a flat-fine-mesh grid by an electrostatic zoom lens consisting of repeller, extractor and ground electrodes. With this arrangement, Eppink and Parker [16] report that ions with identical velocities produced anywhere within the interaction volume can be spatially focused to a very small "spot" on the detector ($\sim 150\,\mu m$). In the course of this work, because of the limited spatial resolution offered by the microsphere plates (El Mul) used in our detector, we have been able to achieve only moderate "ion-spot" sizes of $\sim 800$ μm. Even so, we find that the energy resolution of our spectrometer is improved to about 10%, from 20% when the grid is used [15].

## RESULTS/DISCUSSION

The Cl and Cl* photofragments are ionized using two-photon resonant transitions $4p(^4D_{5/2}) \leftarrow 3p^5(^2P_{1/2})$ at 240.19 nm and the $4p(^4P_{3/2}) \leftarrow 3p^5(^2P_{3/2})$ 240.53 [10, 17, 18]. Data images representing the 2D projection of the 3D velocity distributions for the photofragments $^{35}Cl^*$ and $^{35}Cl$ are shown in Figures 1(a, b). Both data images are averaged with respect to the symmetry axis (laser polarization direction) and subsequently averaged with respect to an axis perpendicular to the laser polarization direction which passes through the center-of-mass.

The angular distributions for Cl* and Cl photofragments shown in Figures 2(a, b), are determined by appropriate processing [13, 19], of the images in Figures 1(a, b). Both distributions are strongly anisotropic, peaking at $\theta = 90°$. Modeling the experimental angular distribution presented in Figure 2(a) using the functional form of Eq. (1)

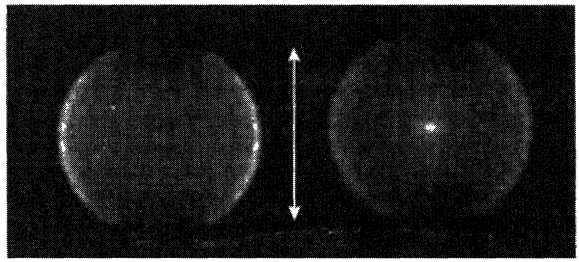


FIGURE 1 (a) Data image of the $Cl(^2P_{3/2})$ photofragment; (b) Data image of the $Cl(^2P_{1/2})$ photofragment generated from the photodissociation of $Cl_2$ at 308 nm. The polarization direction of the photolysis laser is indicated by the arrow. The bright spot at the center of image (b) is $Cl^*$ from the photodissociation of $(Cl_2)_{N=2,3,\ldots}$ clusters.

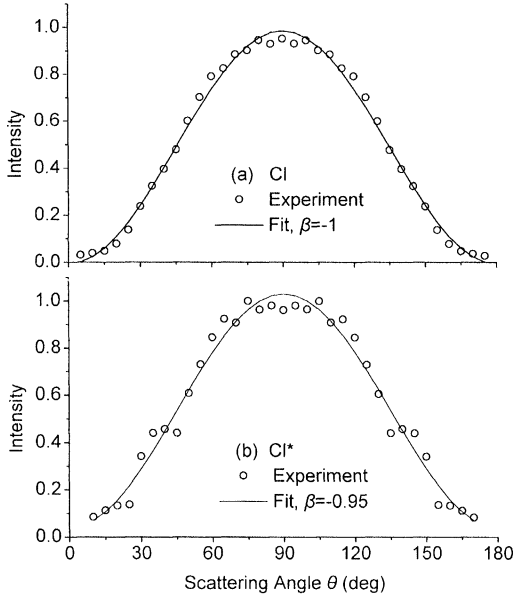


FIGURE 2 Angular distribution for the $Cl(^2P_{1/2})$, $Cl(^2P_{3/2})$ photofragments generated from the photodissociation of $Cl_2$ at 308 nm.

we find that $\beta(Cl) = -1.00 \pm 0.05$. This values implies a prompt dissociation following excitation through a perpendicular transition [6, 7] such as $1_u \leftarrow 0_g^+(X^1\Sigma_g)$. The disturbing result concerns the

value $\beta(Cl^*) = -0.95 + 0.05$ determined by fitting the data show in Figure 2(b). This result is surprising because $Cl^*$ is produced exclusively by the parallel excitation $0_u^+ \leftarrow 0_g^+(X^1\Sigma_g)$ and hence, upon prompt dissociation this process should yield a $\cos^2\theta$ distribution (*i.e.*, $\beta(Cl^*) = 2.0$). Previous measurements of the Cl and $Cl^*$ angular distribution at this wavelength reported $\beta(Cl^*) = -0.7 \pm 0.2$ and $\beta(Cl) = -1 \pm 0.1$ [4, 11], in fair agreement with our results.

The "anomalous" $\beta(Cl^*)$ value is attributed to non-adiabatic curve-crossing between the $1_u$ and the $0_u^+$ electronic states. From the $Cl^*$ image, we can determine the ratio of direct *vs* indirect $Cl^*$ production (100% direct production implies $\beta(Cl^*) = 2.0$, while 100% indirect production via curve crossing yields $\beta(Cl^*) = -1.0$). From the experimentally determined value $\beta(Cl^*) = -0.95$, we conclude that

$$\frac{Cl^*_{\text{indirect}}}{Cl^*_{\text{direct}} + Cl^*_{\text{indirect}}} \approx 98\%,$$

*i.e.*, $Cl^*$ is essentially produced via non-adiabatic curve crossing. Determining the magnitude of this curve crossing probability is in principle possible from the Cl image, as two rings are anticipated, one corresponding to Cl + Cl, and the other to $Cl^* + Cl$. Unfortunately, the energy resolution of our spectrometer ($\sim$10%) is not sufficient to resolve these two rings.

## *Acknowledgements*

This work is supported by the General Secretariat for Research and Technology under the program PENED94 and is conducted at the Ultraviolet Laser Facility operating at FORTH-IESL (Human Capital and Mobility, Access to Large Scale Facilities EU program, Contract No. CHGE-CT92-007).

## *References*

[1] Mulliken, R. S. (1930). *Phys. Rev.*, **36**, 1440.
[2] Herzberg, G., Molecular Spectra and Molecular Structure I, Spectra of Diatomic Molecules (Van Nostrand Reihnhold, NY, 1950), pp. 319–322.
[3] Li, L., Lipert, R. J., Lobue, J., Chupka, W. A. and Colson, S. D. (1988). *Chem. Phys. Lett.*, **151**, 335.

[4] Matsumi, Y., Tonokura, K. and Kawasaki, M. (1992). *J. Chem. Phys.*, **97**, 1065.
[5] Ref. 2, p. 224.
[6] Zare, R. N. (1972). *Mol. Photochem.*, **4**, 1.
[7] Yang, S. and Bersohn, R. (1974). *J. Chem. Phys.*, **61**, 4400.
[8] Busch, G. E., Mahoney, R. T., Morse, R. I. and Wilson, K. R. (1969). *J. Chem. Phys.*, **51**, 449.
[9] Diesen, R. W., Wahr, J. C. and Adler, S. E. (1969). *J. Chem. Phys.*, **50**, 3635.
[10] Arepalli, S., Presser, N., Robie, D. and Gordon, R. J. (1985). *Chem. Phys. Lett.*, **118**, 88.
[11] Matsumi, Y., Kawasaki, M., Sato, T., Kinugawa, T. and Arikawa, T. (1989). *Chem. Phys. Lett.*, **155**, 486.
[12] Chandler, D. W. and Houston, P. L. (1987). *J. Chem. Phys.*, **87**, 1445.
[13] Heck, A. J. R. and Chandler, D. W. (1995). *Annu. Rev. Phys. Chem.*, **46**, 335.
[14] Houston, P. L. (1996). *J. Phys. Chem.*, **100**, 12757.
[15] Samartzis, P. C., Sakellariou, I., Gougousi, T. and Kitsopoulos, T. N. (1997). *J. Chem. Phys.*, **107**, 43.
[16] Eppink, A. T. J. B. and Parker, D. H. (1997). *Rev. Sci. Instrum.*, **68**, 3477.
[17] Simpson, W. R., Rakitzis, T. P., Kandel, A. A., Orr-Ewing, J. and Zare, R. N. (1995). *J. Chem. Phys.*, **103**, 7313.
[18] Moore, C. E., Atomic Energy Levels as derived from the analyses of optical spectra (Washington, U.S. Dept. of Commerce, National Bureau of 1949).
[19] Chandler, D. W., Kitsopoulos, T. N., Buntine, M. A., Baldwin, D. P., McKay, R. I., Heck, A. J. R. and Zare, R. N., Gas-Phase Chemical Reaction Systems: Experiments and Models 100 Years after Max Bodenstein, Eds. Wolfrum, J., Volpp, H.-R., Rannacher, R. and Warnatz, J. (Springer Series in *Chem. Phys.*, Springer Berlin, Heidelberg 1996).